

# Generating Mesoscopic Bell States via Collisions of Distinguishable Quantum Bright Solitons

Bettina Gertjerenken,<sup>1</sup> Thomas P. Billam,<sup>2</sup> Caroline L. Blackley,<sup>3</sup> C. Ruth Le Sueur,<sup>3</sup> Lev Khaykovich,<sup>4</sup>  
Simon L. Cornish,<sup>5</sup> and Christoph Weiss<sup>5,\*</sup>

<sup>1</sup>*Institut für Physik, Carl von Ossietzky Universität, D-26111 Oldenburg, Germany*

<sup>2</sup>*Department of Physics, Jack Dodd Center for Quantum Technology, University of Otago, Dunedin 9016, New Zealand*

<sup>3</sup>*Department of Chemistry, Joint Quantum Centre (JQC) Durham-Newcastle, Durham University, Durham DH1 3LE, United Kingdom*

<sup>4</sup>*Department of Physics, Bar-Ilan University, Ramat-Gan 52900, Israel*

<sup>5</sup>*Department of Physics, Joint Quantum Centre (JQC) Durham-Newcastle, Durham University, Durham DH1 3LE, United Kingdom*

(Received 4 January 2013; published 6 September 2013)

We investigate numerically the collisions of two distinguishable quantum matter-wave bright solitons in a one-dimensional harmonic trap. We show that such collisions can be used to generate mesoscopic Bell states that can reliably be distinguished from statistical mixtures. Calculation of the relevant  $s$ -wave scattering lengths predicts that such states could potentially be realized in quantum-degenerate mixtures of  $^{85}\text{Rb}$  and  $^{133}\text{Cs}$ . In addition to fully quantum simulations for two distinguishable two-particle solitons, we use a mean-field description supplemented by a stochastic treatment of quantum fluctuations in the soliton's center of mass: we demonstrate the validity of this approach by comparison to a mathematically rigorous effective potential treatment of the quantum many-particle problem.

DOI: [10.1103/PhysRevLett.111.100406](https://doi.org/10.1103/PhysRevLett.111.100406)

PACS numbers: 03.75.Lm, 03.75.Gg, 03.75.Mn, 67.85.-d

Generating quantum entanglement between mesoscopic objects over mesoscopic distances allows the exploration of a fascinating “middle ground” between quantum and classical physics [1,2] and promises significant advances in quantum-enhanced interferometry [3]. The high degree of experimental control offered by quantum-degenerate gases makes them an ideal platform with which to explore such multiparticle entanglement [4,5]. From a fundamental perspective, the creation of *maximally entangled* many-particle Bell states in quantum-degenerate gases presents an intriguing proposition. The generation of similar macroscopic Bell states of many photons is an area of current theoretical and experimental research [6,7]. In addition to their inherent fundamental interest, such states have potential application as a resource in the area of quantum information [7].

Previously, the scattering of quantum bright matter-wave solitons [8–17] in quasi-one-dimensional (1D) trapping geometries has been suggested as a way to create mesoscopic entangled states in single-species Bose-Einstein condensates (BECs) [13,18,19]. In this Letter, we consider a dual-species BEC [20,21] and show that collisions of distinguishable quantum bright matter-wave solitons can be used to generate mesoscopic Bell states [22] (cf. Ref. [23]),

$$|\psi_{\text{Bell}}\rangle \equiv \frac{1}{\sqrt{2}}(|A, B\rangle + e^{i\alpha}|B, A\rangle), \quad (1)$$

where  $|A, B\rangle$  ( $|B, A\rangle$ ) signifies that the BEC  $A$  is on the left (right) and the BEC  $B$  is on the right (left). In particular, we show that a favorable combination of inter- and intraspecies  $s$ -wave scattering lengths means that such states may be realized using  $^{85}\text{Rb}$  and  $^{133}\text{Cs}$  mixtures. We also show

that the interference properties of these bright-soliton Bell states distinguish them from statistical mixtures. In contrast to the Bell ground states associated with double-well potentials, our collisionally generated Bell states are robust to the presence of asymmetries. While distinguishable solitons are essential to produce Bell states, entanglement generation for solitons of the same species was investigated in Ref. [13].

For our quasi-1D system, we consider an experimentally motivated harmonic confinement  $\omega = 2\pi f$ . Mixtures of ultracold gases can be confined in a common optical trap with the same trap frequencies [24], yielding

$$\omega = \frac{2\pi}{T}; \quad \lambda_A = \sqrt{\frac{\hbar}{m_A\omega}}; \quad \lambda_B = \sqrt{\frac{\hbar}{m_B\omega}}, \quad (2)$$

where  $m_A$  ( $m_B$ ) is the atomic mass of species  $A$  ( $B$ ); the interactions  $g = \hbar f_{\perp} a$  are set by the scattering lengths  $a$  and the perpendicular trapping-frequency,  $f_{\perp}$  [25].

We use the Lieb-Liniger model [26] for two species with additional harmonic confinement

$$\begin{aligned} \hat{H} = & - \sum_{j=1}^{N_A} \frac{\hbar^2}{2m_A} \partial_{x_j}^2 + \sum_{j=1}^{N_A-1} \sum_{n=j+1}^{N_A} g_A \delta(x_j - x_n) \\ & - \sum_{j=1}^{N_B} \frac{\hbar^2}{2m_B} \partial_{y_j}^2 + \sum_{j=1}^{N_B-1} \sum_{n=j+1}^{N_B} g_B \delta(y_j - y_n) \\ & + \sum_{j=1}^{N_A} \sum_{n=1}^{N_B} g_{AB} \delta(x_j - y_n) + \sum_{j=1}^{N_A} \frac{1}{2} m_A \omega^2 x_j^2 \\ & + \sum_{j=1}^{N_B} \frac{1}{2} m_B \omega^2 y_j^2, \end{aligned} \quad (3)$$

where  $x_j$  ( $y_j$ ) and  $g_A < 0$  ( $g_B < 0$ ) are the atomic coordinates and intraspecies interactions of species  $A$  ( $B$ ), and  $g_{AB} \geq 0$  is the interspecies interaction.

We suggest to prepare the two solitons independently; for weak harmonic confinement a single soliton has the ground-state energy (cf. Ref. [27])

$$E_S(N_S) = -\frac{1}{24} \frac{m_S g_S^2}{\hbar^2} N_S (N_S^2 - 1); \quad S \in \{A, B\}. \quad (4)$$

Thus, our system has the total ground-state energy

$$E_0 = E_A(N_A) + E_B(N_B). \quad (5)$$

The total kinetic energy related to the center-of-mass momenta  $\hbar K_S$  ( $S \in \{A, B\}$ ) of the two solitons reads

$$E_{\text{kin}} = \frac{\hbar^2 K_A^2}{2N_A m_A} + \frac{\hbar^2 K_B^2}{2N_B m_B}. \quad (6)$$

We extend the low-energy regime investigated for single-species solitons in Refs. [12,18,28] to two species

$$E_{\text{kin}} < \min\{\Delta_A, \Delta_B\}, \quad \Delta_S = |E_S(N_S - 1) - E_S(N_S)|.$$

In this energy regime, each of the quantum matter-wave bright solitons is energetically forbidden to break up into two or more parts. Highly entangled states are characterized by a roughly 50:50 chance of finding the soliton  $A$  ( $B$ ) on the left or the right, combined with a left-right correlation close to one indicating that whenever soliton  $A$  is on the one side, soliton  $B$  is on the other:

$$\begin{aligned} \gamma(\delta) \equiv & \int_{\delta}^{\infty} dx_1 \dots \int_{\delta}^{\infty} dx_{N_A} \int_{-\infty}^{-\delta} dy_1 \dots \int_{-\infty}^{-\delta} dy_{N_B} |\Psi|^2 \\ & + \int_{-\infty}^{-\delta} dx_1 \dots \int_{-\infty}^{-\delta} dx_{N_A} \int_{\delta}^{\infty} dy_1 \dots \int_{\delta}^{\infty} dy_{N_B} |\Psi|^2, \end{aligned} \quad (7)$$

where  $\Psi = \Psi(x_1, \dots, x_{N_A}, y_1, \dots, y_{N_B})$  is the many-particle wave function (normalized to 1) and  $\delta \geq 0$ . The correlation  $\gamma(\delta)$  will serve as an indication of entanglement: Bell states (1) are characterized by  $\gamma \simeq 1$  combined with a 50:50 chance to find soliton  $A$  either on one side or on the other.

We begin by investigating entanglement-generating collisions of two distinguishable two-particle solitons (dimers). Discarding cases where the two solitons have distinct total masses  $N_A m_A$  and  $N_B m_B$  (small differences in the total masses would introduce small asymmetries without changing the physics) leads to  $m_A = m_B = m$ , which corresponds to having two hyperfine states of the same species. To describe the collisions of the two dimers, we discretize the Hamiltonian (3), yielding the Bose-Hubbard Hamiltonian (cf. Ref. [29])

$$\begin{aligned} \hat{H}_{\text{BH}} = & \sum_{\ell} \left\{ \frac{U_A}{2} \hat{a}_{\ell}^{\dagger} \hat{a}_{\ell}^{\dagger} \hat{a}_{\ell} \hat{a}_{\ell} + \frac{U_B}{2} \hat{b}_{\ell}^{\dagger} \hat{b}_{\ell}^{\dagger} \hat{b}_{\ell} \hat{b}_{\ell} \right. \\ & + U_{AB} \hat{a}_{\ell}^{\dagger} \hat{a}_{\ell} \hat{b}_{\ell}^{\dagger} \hat{b}_{\ell} - J(\hat{a}_{\ell}^{\dagger} \hat{a}_{\ell+1} + \hat{a}_{\ell+1}^{\dagger} \hat{a}_{\ell} \\ & \left. + \hat{b}_{\ell}^{\dagger} \hat{b}_{\ell+1} + \hat{b}_{\ell+1}^{\dagger} \hat{b}_{\ell}) + C \ell^2 \hat{a}_{\ell}^{\dagger} \hat{a}_{\ell} + C \ell^2 \hat{b}_{\ell}^{\dagger} \hat{b}_{\ell} \right\}, \quad (8) \end{aligned}$$

where  $U_A$ ,  $U_B$ , and  $U_{AB}$  are the intraspecies and interspecies interactions, the hopping is given by  $J \sim \hbar^2/(2md^2)$  for grid spacing  $d \rightarrow 0$ , and  $C \equiv 0.5m\omega^2 d^2$ .

Figure 1 shows two-dimensional projections of the dynamics of two distinguishable dimers. The two dimers were numerically prepared in the ground state of two spatially separated harmonic oscillators via imaginary time evolution [30]. At time  $t = 0$ , they were transferred into the same harmonic oscillator potential (without overlap). Subsequently, the time evolution was calculated using the full Schrödinger equation corresponding to the Hamiltonian (8). After the first collision, a measurement would reveal dimer  $A$  on the left and dimer  $B$  on the right or vice versa [the correlation (7) is  $\gamma(d/2) \simeq 0.988$ ].

As the sizes of the dimers in panels Figs. 1(a) and 1(b) are not too large compared to the oscillator length, after the second collision both dimers are more likely to be on the side opposite to their initial condition than at the same side (cf. the single soliton case [28]). This can be used to distinguish a pure quantum superposition from a statistical

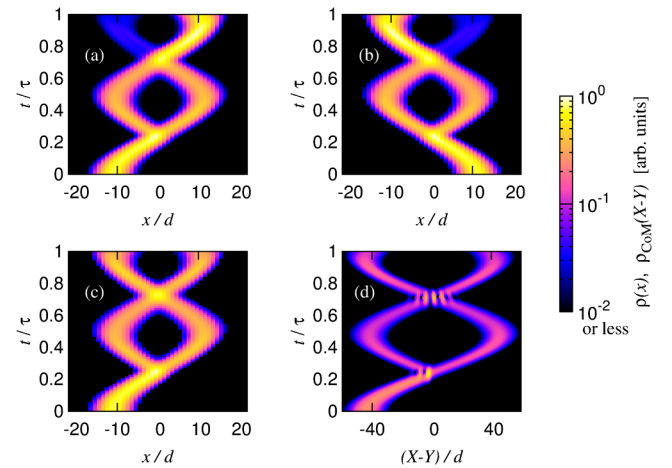


FIG. 1 (color online). Collisions of two distinguishable dimers in the Bose-Hubbard Hamiltonian (8). (a) Single-particle density  $\varrho(x)$  of dimer  $A$  in a two-dimensional projection as a function of space and time ( $\tau$  is the oscillation period without interspecies interaction,  $U_A = -3J$ ,  $U_B = -3J$ ,  $U_{AB} = J$ , and  $C = 0.002J$ ). (b) Single-particle density of dimer  $B$ , with parameters as in panel (a). (c) The same dimer as in panel (a) but with the wave function numerically turned into a statistical mixture at  $t = \tau/2$ . (d) Center-of-mass density  $\varrho_{\text{COM}}(X-Y)$  if the interspecies interaction is switched off at  $t = \tau/2$ , with all other parameters as in (a) and (b). The interference pattern near  $t = 0.7\tau$ , combined with a high correlation (7) of  $\gamma(d/2) \simeq 0.988$  near  $t = 0.5\tau$ , indicates that a Bell state has been created.

mixture [Fig. 1(c)]. A more general approach extends the center-of-mass density [31] to two solitons [Fig. 1(d)]: after switching off the interspecies interaction when the Bell state has formed, one first measures the center of mass  $X$  and  $Y$  of solitons  $A$  and  $B$  and then plots the resulting density  $\varrho_{\text{CoM}}$  as a function of the difference  $X - Y$ . This works both for superpositions of plane waves  $\exp[iKX]\exp[-iKY] + \exp[-iKX]\exp[iKY]$  with

$$\varrho_{\text{CoM}}(X - Y) \propto \{\cos[K(X - Y)]\}^2 \quad (9)$$

and when the two wave packets recombine [Fig. 1(d)]. Measuring a contrast close to one as in Eq. (9) is possible as the center of mass can be measured with higher accuracy than the soliton width (cf. Ref. [31]). As shown in Ref. [31] for the single-species case, CoM interferences do, in general, not correspond to interferences in single-particle densities that have been investigated, e.g., for distinguishable BECs in Ref. [32].

To show that attractive intraspecies interactions and repulsive, *tunable* interspecies interactions are experimentally feasible, we calculate the  $s$ -wave scattering lengths for  $^{85}\text{Rb}^{133}\text{Cs}$ . The results displayed in Fig. 2 shows a candidate interspecies Feshbach resonance at 6.76 G suitable for our requirements [33]. For lower magnetic fields, the magnetic field can be stabilized to up to 100  $\mu\text{G}$  [34]; shielding allows stabilization to 1 mG below 10 G. Although the masses of the atoms  $A$  and  $B$  now differ, we can still have two solitons of roughly the same total masses  $N_A m_A$  and  $N_B m_B$  as in Fig. 1.

Behavior for larger particle numbers can be described by the Gross-Pitaevskii equation (GPE) (cf. [35–38])

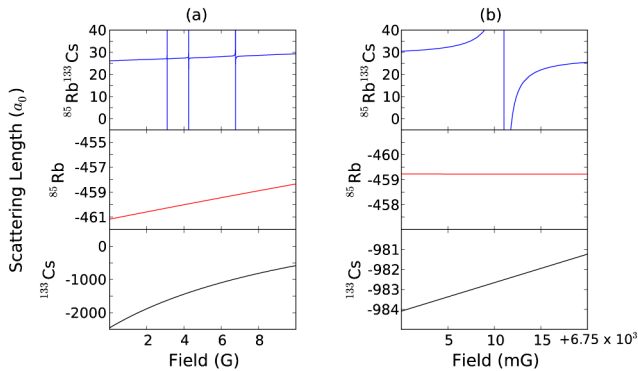


FIG. 2 (color online). The  $s$ -wave scattering lengths for the ground state of  $^{85}\text{Rb}^{133}\text{Cs}$ ,  $^{85}\text{Rb}$ , and  $^{133}\text{Cs}$  respectively. (a) Scattering lengths are calculated using a coupled-channels method [21] with a fully decoupled basis set at a collision energy of 1 pK. The calculations are performed using the MOLSCAT program [45] adapted to handle collisions in external fields [46]. The RbCs potential is from Ref. [21], the Rb potential is from Ref. [47], and the Cs potential is from Ref. [48]. Resonances for  $^{85}\text{Rb}^{133}\text{Cs}$  are at 3.10, 4.27, and 6.76 G [33]. (b) Zoom view of (a).

$$\begin{aligned} i\hbar\partial_t\varphi_A(x, t) &= \left[ -\frac{\hbar^2}{2m_A}\partial_x^2 + \frac{g_A}{2}|\varphi_A(x, t)|^2 \right] \varphi_A(x, t) \\ &\quad + \left[ \frac{1}{2}m_A\omega^2x^2 + \frac{g_{AB}}{2}|\varphi_B(x, t)|^2 \right] \varphi_A(x, t), \\ i\hbar\partial_t\varphi_B(x, t) &= \left[ -\frac{\hbar^2}{2m_B}\partial_x^2 + \frac{g_B}{2}|\varphi_B(x, t)|^2 \right] \varphi_B(x, t) \\ &\quad + \left[ \frac{1}{2}m_B\omega^2x^2 + \frac{g_{AB}}{2}|\varphi_A(x, t)|^2 \right] \varphi_B(x, t), \end{aligned}$$

where the single-particle density  $|\varphi_S(x, t)|^2$  is normalized to  $N_S$  ( $S \in \{A, B\}$ ).

When hitting a barrier, the generic behavior of a mean-field bright soliton is to break into two parts; the fraction of the atoms transmitted decreases for increasing potential strength (cf. Refs. [15,17]). An analogous behavior also occurs when two mean-field bright solitons hit each other as shown in the Supplemental Material [39].

Low kinetic energies generate very different GPE dynamics. For the case of a single-species soliton incident upon a potential barrier, one observes a sharp stepwise jump in the GPE reflection coefficient as a function of barrier height [16,28,40]. In this case we previously [28] showed that this jump occurs in regimes where, on the  $N$ -particle quantum level, the low kinetic energies prevent the soliton from breaking into two (or more) smaller solitons and thus provides a useful GPE-level indicator for the formation of  $N$ -particle quantum superpositions.

Conjecturing that sharp stepwise jumps in the GPE reflection coefficient for distinguishable soliton collisions may indicate Bell states, we investigate parameters yielding such jumps (cf. Supplemental Material [39]). To confirm that these jumps indicate Bell state formation, we use the truncated-Wigner approximation (TWA), which describes quantum systems by averaging over realizations of an appropriate classical field equation (in this case, the GPE) with initial noise appropriate to either finite [41] or zero temperatures [15]. Whereas the GPE assumes that both position and momentum are well defined, this is not true for a single quantum particle of finite mass for which, in general, both position and momentum involve quantum noise satisfying the uncertainty relation. Our TWA calculations for the soliton center-of-mass wave function use Gaussian probability distributions for both (satisfying minimal uncertainty).

To demonstrate that the center-of-mass TWA is indeed a valid approach to describe the short-time behavior of mesoscopic quantum superpositions, Fig. 3 starts with the case where a light soliton hits a heavy, nonmoving soliton. In Fig. 3(a), the rigorously proved [42] effective potential approach [12,18,43] demonstrates the emergence of a Schrödinger-cat state when the GPE predicts the stepwise behavior of the reflection coefficient explained in Refs. [16,28,40] [Fig. 3(c)].

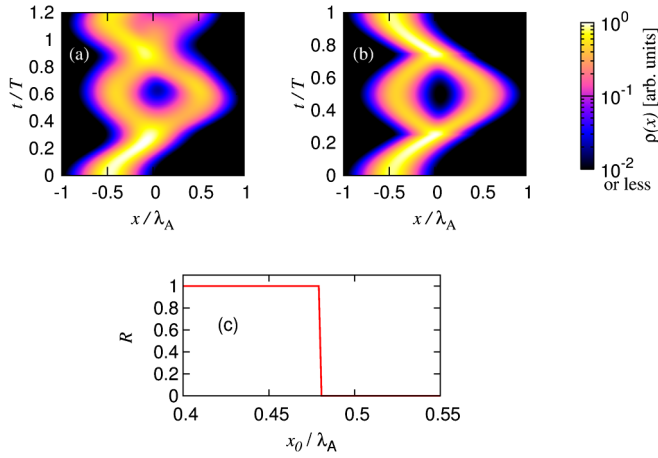


FIG. 3 (color online). (a) Single-particle density for an  $N$ -particle quantum bright soliton hitting a narrow, heavy non-moving soliton, computed using the effective potential approach [43]. (b) As in (a) but using the TWA for the center of mass. The parameters are in the low-kinetic-energy regime such that the GPE predicts a sharp stepwise [28] behavior of reflection coefficient as a function of the initial displacement shown in panel (c);  $U_0 \approx 12\hbar\omega$  (cf. Ref. [43]).

In Fig. 3(b), we use the TWA to average over the analytic approximation for the classical-particle-like behavior of the GPE soliton [44]. This leads to a good qualitative agreement with the  $N$ -particle predictions in Fig. 3(a) up to the time where both parts of the wave function recombine and quantum interference becomes important.

On the  $N$ -particle level, the low kinetic energies are important for the soliton not to be able to break into two (or more) smaller solitons. Whereas GPE solitons can, during a collision, lose a small fraction of particles, for low kinetic energies this effect becomes negligible [24]. Thus, the sharp stepwise behavior shown in Fig. 3(c) leads to a behavior very close to the true  $N$ -particle quantum case.

In order to observe Bell states, we investigate two distinguishable bright solitons of similar mass at low kinetic energy ( $E_{\text{kin}}/|E_0| = 0.182$ ). Applying the TWA for the center-of-mass wave functions of both solitons leads to the single-particle densities displayed in Figs. 4(a) and 4(b). The low kinetic energies indicate that the feature shown in those single-particle densities near  $t \approx 0.6T$  should indeed be a Bell state. The value of the correlation function close to 1 [Fig. 4(c)] shows that we indeed have found a Bell state. Whereas the TWA is no longer valid as soon as both parts of the wave function overlap, a full quantum mechanical calculation would also lead to a decrease of the correlation in Fig. 4(c) on this time scale.

To conclude, on the basis of predictions made on the level of many-particle quantum calculations (using the Lieb-Liniger model), we demonstrated numerically that mesoscopic Bell states can be generated by colliding two distinguishable quantum matter-wave bright solitons.

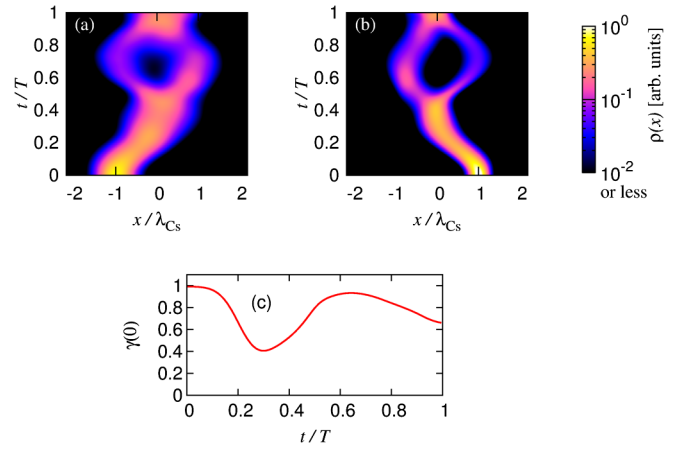


FIG. 4 (color online). TWA for the center of mass in the low-kinetic-energy regime applied to the two-species GPE. The single-particle density for the  $^{133}\text{Cs}$  soliton is displayed in panel (a) and for  $^{85}\text{Rb}$  in panel (b). (c) This leads to a correlation (7) close to 1, thus indicating a Bell state. Parameters:  $a_{\text{Cs}} = -982.5a_0$ ,  $a_{\text{Rb}} = -459.2a_0$ ,  $f = 1 \text{ Hz}$ ,  $f_{\perp} = 70 \text{ Hz}$ ,  $N_{\text{Cs}} \approx 12$ ,  $N_{\text{Rb}} \approx 19$  (corresponding to  $N_{\text{Rb}}m_{\text{Rb}} \approx N_{\text{Cs}}m_{\text{Cs}}$ , thus avoiding center-of-mass movement),  $a_{\text{RbCs}} = 63.6a_0$ , and the initial displacement from trap center is  $-8.7 \mu\text{m}$  for  $^{133}\text{Cs}$  and  $+8.7 \mu\text{m}$  for  $^{85}\text{Rb}$ .

In experiment, the formation of these states could be confirmed by switching off the interspecies interaction once the Bell state has formed and then measuring the interference fringes in the combined center-of-mass density (9) (see Fig. 1), revealing the presence of quantum superposition. Finally, we have shown that matter-wave bright solitons in  $^{85}\text{Rb}$ - $^{133}\text{Cs}$  mixtures are a promising candidate system for the experimental realization of mesoscopic Bell states, presenting an intriguing target for future experimental investigations.

We thank C.S. Adams, S.A. Gardiner, J.L. Helm, J.M. Hutson, and M.P. Köpinger for discussions. We thank the Studienstiftung des deutschen Volkes (B.G.), the Heinz Neumüller Stiftung (B.G.), the Marsden Fund of New Zealand (Contract No. UOO162) and the Royal Society of New Zealand (Contract No. UOO004) (T.P.B.), the Faculty of Science at Durham University (C.L.B.), the EOARD (Grant No. FA8655-10-1-3033) (C.R.L.S.), and the UK EPSRC (Grant No. EP/G05 6781/1) (C.W.) for funding.

\*Christoph.Weiss@durham.ac.uk

- [1] L. Hackermüller, K. Hornberger, B. Brezger, A. Zeilinger, and M. Arndt, *Nature (London)* **427**, 711 (2004).
- [2] W.H. Zurek, *Rev. Mod. Phys.* **75**, 715 (2003).
- [3] V. Giovannetti, S. Lloyd, and L. Maccone, *Science* **306**, 1330 (2004).
- [4] J. Estève, C. Gross, A. Weller, S. Giovanazzi, and M.K. Oberthaler, *Nature (London)* **455**, 1216 (2008).

- [5] M. F. Riedel, P. Böhi, Y. Li, T. W. Hänsch, A. Sinatra, and P. Treutlein, *Nature (London)* **464**, 1170 (2010).
- [6] M. Stobińska, F. Töppel, P. Sekatski, and M. V. Chekhova, *Phys. Rev. A* **86**, 022323 (2012).
- [7] T. S. Iskhakov, I. N. Agafonov, M. V. Chekhova, and G. Leuchs, *Phys. Rev. Lett.* **109**, 150502 (2012).
- [8] L. Khaykovich, F. Schreck, G. Ferrari, T. Bourdel, J. Cubizolles, L. D. Carr, Y. Castin, and C. Salomon, *Science* **296**, 1290 (2002).
- [9] K. E. Strecker, G. B. Partridge, A. G. Truscott, and R. G. Hulet, *Nature (London)* **417**, 150 (2002).
- [10] H. Buljan, M. Segev, and A. Vardi, *Phys. Rev. Lett.* **95**, 180401 (2005).
- [11] S. L. Cornish, S. T. Thompson, and C. E. Wieman, *Phys. Rev. Lett.* **96**, 170401 (2006).
- [12] K. Sacha, C. A. Müller, D. Delande, and J. Zakrzewski, *Phys. Rev. Lett.* **103**, 210402 (2009).
- [13] M. Lewenstein and B. A. Malomed, *New J. Phys.* **11**, 113014 (2009).
- [14] T. Ernst and J. Brand, *Phys. Rev. A* **81**, 033614 (2010).
- [15] A. D. Martin and J. Ruostekoski, *New J. Phys.* **14**, 043040 (2012).
- [16] S. D. Hansen, N. Nygaard, and K. Mølmer, [arXiv:1210.1681](https://arxiv.org/abs/1210.1681).
- [17] J. Cuevas, P. G. Kevrekidis, B. A. Malomed, P. Dyke, and R. G. Hulet, *New J. Phys.* **15**, 063006 (2013).
- [18] C. Weiss and Y. Castin, *Phys. Rev. Lett.* **102**, 010403 (2009).
- [19] A. I. Streltsov, O. E. Alon, and L. S. Cederbaum, *Phys. Rev. A* **80**, 043616 (2009).
- [20] D. J. McCarron, H. W. Cho, D. L. Jenkin, M. P. Köppinger, and S. L. Cornish, *Phys. Rev. A* **84**, 011603 (2011).
- [21] T. Takekoshi, M. Debatin, R. Rameshan, F. Ferlaino, R. Grimm, H.-C. Nägerl, C. R. Le Sueur, J. M. Hutson, P. S. Julienne, S. Kotochigova, and E. Tiemann, *Phys. Rev. A* **85**, 032506 (2012).
- [22] G. Csire and B. Apagyí, *Phys. Rev. A* **85**, 033613 (2012).
- [23] M. A. Garcia-March, D. R. Dounas-Frazer, and L. D. Carr, *Phys. Rev. A* **83**, 043612 (2011).
- [24] M. S. Safronova, B. Arora, and C. W. Clark, *Phys. Rev. A* **73**, 022505 (2006).
- [25] M. Olshanii, *Phys. Rev. Lett.* **81**, 938 (1998).
- [26] E. H. Lieb and W. Liniger, *Phys. Rev.* **130**, 1605 (1963).
- [27] J. B. McGuire, *J. Math. Phys. (N.Y.)* **5**, 622 (1964).
- [28] B. Gertjerenken, T. P. Billam, L. Khaykovich, and C. Weiss, *Phys. Rev. A* **86**, 033608 (2012).
- [29] E. Altman, W. Hofstetter, E. Demler, and M. D. Lukin, *New J. Phys.* **5**, 113 (2003).
- [30] J. A. Glick and L. D. Carr, [arXiv:1105.5164](https://arxiv.org/abs/1105.5164).
- [31] B. Gertjerenken and C. Weiss, *J. Phys. B* **45**, 165301 (2012).
- [32] L. S. Cederbaum, A. I. Streltsov, Y. B. Band, and O. E. Alon, *Phys. Rev. Lett.* **98**, 110405 (2007).
- [33] H.-W. Cho, D. J. McCarron, M. P. Köppinger, D. L. Jenkin, K. L. Butler, P. S. Julienne, C. L. Blackley, C. R. Le Sueur, J. M. Hutson, and S. L. Cornish, *Phys. Rev. A* **87**, 010703 (R) (2013).
- [34] B. Pasquiou, E. Maréchal, L. Vernac, O. Gorceix, and B. Laburthe-Tolra, *Phys. Rev. Lett.* **108**, 045307 (2012).
- [35] H. Pu and N. P. Bigelow, *Phys. Rev. Lett.* **80**, 1134 (1998).
- [36] E. Timmermans, *Phys. Rev. Lett.* **81**, 5718 (1998).
- [37] P. Öhberg and L. Santos, *Phys. Rev. Lett.* **86**, 2918 (2001).
- [38] Z. M. He, D. L. Wang, J. W. Ding, and X. H. Yan, *Eur. Phys. J. D* **66**, 139 (2012).
- [39] See Supplemental Material at <http://link.aps.org/supplemental/10.1103/PhysRevLett.111.100406> to see that bright solitons break apart during collisions at higher kinetic energies and only behave similar to a big molecule for low kinetic energies.
- [40] C.-H. Wang, T.-M. Hong, R.-K. Lee, and D.-W. Wang, *Opt. Express* **20**, 22675 (2012).
- [41] P. Bienias, K. Pawłowski, M. Gajda, and K. Rzazewski, *Europhys. Lett.* **96**, 10011 (2011).
- [42] C. Weiss and Y. Castin, *J. Phys. A* **45**, 455306 (2012).
- [43] This approach replaces the  $N$ -particle Schrödinger equation by a single-particle Schrödinger equation for the center-of-mass coordinate. The effective potential is the convolution of the soliton with the potential seen by single particles [12,18], in our case the soliton  $B$  which is chosen to be a factor of  $N_B g_B / (N_A g_A) = 10$  narrower than soliton  $A$ :  $U_1 [\cosh(N_B g_B x)]^{-2} \approx 2U_1 / (N_B g_B) \delta(x)$ . If soliton  $A$  hits the narrow soliton  $B$  [Fig. 3(a)], the effective potential  $U_0 [\cosh(N_A g_A x)]^{-2}$  has the GPE shape of the  $A$  soliton with  $U_0 = N_A U_1 N_A g_A / (N_B g_B) = 10U_1$ , for  $N_A = 100$ .
- [44] A. D. Martin, C. S. Adams, and S. A. Gardiner, *Phys. Rev. A* **77**, 013620 (2008).
- [45] J. M. Hutson and S. Green, MOLSCAT computer program, version 14, distributed by Collaborative Computational Project No. 6 of the UK Engineering and Physical Sciences Research Council, 1994.
- [46] M. L. González-Martínez and J. M. Hutson, *Phys. Rev. A* **75**, 022702 (2007).
- [47] C. Strauss, T. Takekoshi, F. Lang, K. Winkler, R. Grimm, J. Hecker Denschlag, and E. Tiemann, *Phys. Rev. A* **82**, 052514 (2010).
- [48] M. Berninger, A. Zenesini, B. Huang, W. Harm, H.-C. Nägerl, F. Ferlaino, R. Grimm, P. S. Julienne, and J. M. Hutson, *Phys. Rev. Lett.* **107**, 120401 (2011).